Volume 19, Number 2, 2017 

Global Journal of Engineering Education

# Numerical study of the strengthening techniques of Mornos aqueduct - a case study

**Vassilios J. Soulis† & Randa Hattab‡**

School of Pedagogical and Technological Education, Iraklion, Greece†
Piraeus University of Applied Sciences, Piraeus-Athens, Greece‡

ABSTRACT: In March 2011, a failure of Mornos aqueduct in the Athens Water Supply occurred in Central Greece. In the present study, a series of numerical investigations are performed in an effort to find out and propose different strengthening techniques that will raise the horizontal bearing capacity of the aqueduct under study. This study is particularly useful for reducing failures of the aqueduct system in the future and to propose an evaluation tool of the structural performance of relative structures. The external water supply system of Athens includes 189 km of aqueducts, tunnels and siphons that transfer water from the rich rainfall in Western Greece to the city of Athens. The R/C canal aqueduct is formed from articulated segments that are joined together using an interlocking system that adopts protrusions and intrusions in their joint interfaces. This system has suffered the most significant failures along the 40 years of its operation. This methodological approach of the evaluation of the numerical behaviour of the canal, initially studies the numerical behaviour of an original canal section and secondly the performance of the same canal section utilising different strengthening techniques. Finally, a strengthening algorithm is proposed for the evaluation of the strengthening techniques for existing aqueduct systems.

Keywords: Failure mechanism, aqueduct, numerical investigation, non-linear analysis

## INTRODUCTION

Mornos aqueduct is the main water supply system for the city of Athens. The Taxiarches canal of Mornos aqueduct was constructed on pure and dissimilar sub-soil conditions. This situation established differential settlements and excessive earth pressures in particular sections of the aqueduct that caused successive articulated R/C segments to detach. In that sense, the study of the failure that took place at the Taxiarxes canal of Mornos aqueduct is a soil structure interaction problem. Soil structure interaction problems have been studied extensively in the last decade; however, the study of dissimilar sub-soil conditions in respect to their impacts on aqueduct infrastructures is a topic area with great research challenges.

Kotzias and Stamatopoulos in their report summarised the findings of earlier inspections on Taxiarxes canal [1]. The phenomena that were observed could be listed as: overturning of wall segments, settlement of bed plate segments vertical cracks in the joint interfaces between wall segments, significant water outflows in the joints between wall and bed plate segments. Significant horizontal displacements of magnitude of 5 cm were observed in the period 1981-1983 on particular canal walls. In 1989, periodic measurements showed vertical displacement levels of 2 mm.

Mourtzas et al studied the causes of the recent failure at Taxiarches canal that was activated in March 2011 [2]. Their study was based on geological mapping, evaluation of the engineering geological conditions, soil fracture characteristics, the damage to the canal segments and their measured displacements. The study by Mourtzas et al (2013) also included findings that originated from the geotechnical borehole drilling, inclinometers installation and geophysical survey. These findings were retrieved in the current study for evaluation of the numerical behaviour of the aqueduct's simulation. The failure of the canal occurred after intense snow fall, in an area of steep morphology, at the front of an overthrust, within material of reduced mechanical properties, vulnerable to erosion. The soil fracture of the canal foundation caused detachments between segments, outflow of great water quantities and damage to the downstream village of Saranti.

With respect to the factors inducing the above displacements, groundwater hydrostatic pressure below the surveillance road, acting on the hillside (northern) canal wall, is considered critical. Based on the morphology and geology of the area and the time of failure (spring time associated with high water level), it is reasonable to assume that the backfilled soil behind the hillside (northern) wall was saturated and, therefore, the hydrostatic pressure built up on the hillside wall and the buoyancy of the canal bed plate are considered as the major destabilising factors. It is considered that the largest size detachment occurred at the joint area between canal segments No 6 and 7, thus, causing severe soil erosion, which finally led to the occurrence of the main slide (eastern gully, Figure 1 and Figure 2). This hypothesis is considered reasonable, taking into account that the canal curvature is maximised there and, therefore, due to the displacement of adjacent canal segments it would have caused even larger joint detachment. Furthermore, at the area of segments No 6 and 7, the thickness of erodible material (mainly tectonic breccias) is increased, thus, explaining the larger size of the main slide area (eastern gully).


Figure 1: Soil subsidence uphill of the left canal wall between segments 1 and 2 [2].

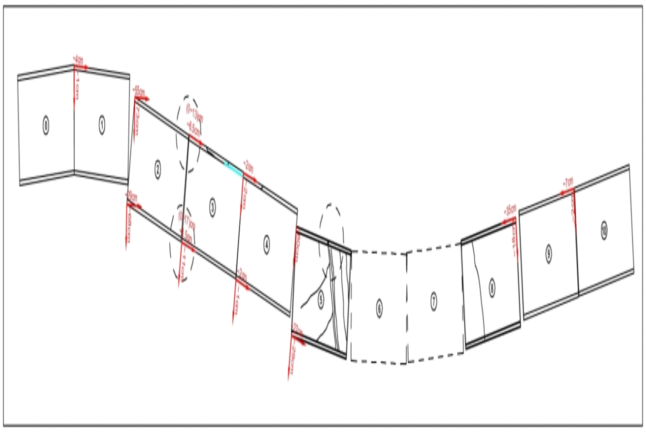

Figure 2: Displacement vectors of canal segments [2].

The El Dorado Irrigation District [3] faces the same problems as the Athens Water Supply and Sewerage Company in their task to conserve the water carrying system that they both supervise. Over the 65-year record, the canal has experienced an average failure incidence rate of 1.4 per year. The causes of these failures include landslides, snow, ice, fire, trees, normal wear and vandals. Certain portions of the canal have had a much higher frequency of failure than others. The likelihood of such failures is higher in wet years and major storm events.

In the current study, a numerical simulation was built in an effort to validate qualitatively the findings of the extensive visual inspection in terms of the kinematics and the failure mechanism of the aqueduct. Furthermore, two strengthening techniques were selected and their influence on the structural behaviour of the aqueduct under study is investigated. The first strengthening scheme introduces beam elements in the top of the *U* shape aqueduct that join the sides of the aqueduct's walls. The second strengthening scheme introduces horizontal anchors that join together the adjacent wall segments of the aqueduct. Finally, an algorithm is proposed that presents the successive steps that must be followed for an optimum design of strengthening schemes.

## STRUCTURAL DESCRIPTION OF R/C CANAL SEGMENTS

The canal segments, walls and the bed plates were constructed from reinforced concrete. The vertical walls were designed as gravity walls with trapezoidal shape. The left wall in respect to the water flow was higher than the right wall. The reason for this design difference is related to the backfill soil conditions of the surveillance road that the left wall was designed to retain. On the contrary, the right wall was adjacent to the steep soil of the original excavation with slope inclination higher than 2:3 (h: b). Later, the right wall was strengthened by the application of pre-stressed steel wires (18Φ4.5/80 cm). The typical geometry of a canal section in the area of failure is shown in Figure 3. The reinforcement details are also shown in Figure 3. In Table 1, the *as built* material properties of the construction materials are listed.

Table 1: *As built* strength of concrete and steel properties for the canal segments.

| Stage of implementation | Class | Young modulus of concrete (N/mm$^2$) | Compressive strength of concrete (N/mm$^2$) | Tensile strength of concrete (N/mm$^2$) |
|---|---|---|---|---|
| Concrete | B160 | 26,000 | 15 | 1.6 |
| Steel | STIV | 200,000 | 500 | |

Table 2: Material strength properties adopted for the numerical analysis.

| Soil-structure interface | | | | | |
|---|---|---|---|---|---|
| A/a | Sub-soil characterisation | E (Mpa) | G (Mpa) | c (Mpa) | Friction coef. |
| Strong sub-soil | Fill-base material | 392 | 163 | 0 | 0.36 |
| Weak sub-soil | Erodible material of overthrusted zone | 50 | 22 | 0 | 0.36 |
| Sliding behaviour between concrete-concrete surfaces | | | | | |
| Concrete-concrete | - | 2,600 | 1,083 | 0.2 | 0.60 |

In Table 2, two sets of soil material properties are presented; one strong and one weak. The strong set of material properties concern the fill–base material properties as originally adopted in the design of the project, and the weak set of material properties concern the soil material in the overthrusted zone (below segments No 6 and 7). In Table 2, the deformability parameters for soil-structure interface are depicted and, more specifically, the young modulus E, the shear modulus G, together with the Poisson's ratio and the coefficient of friction. In the same table the equivalent young modulus E, the shear modulus G, the Poisson's ratio, the cohesion *c* and the friction coefficient values for the concrete to concrete joint interface are presented.

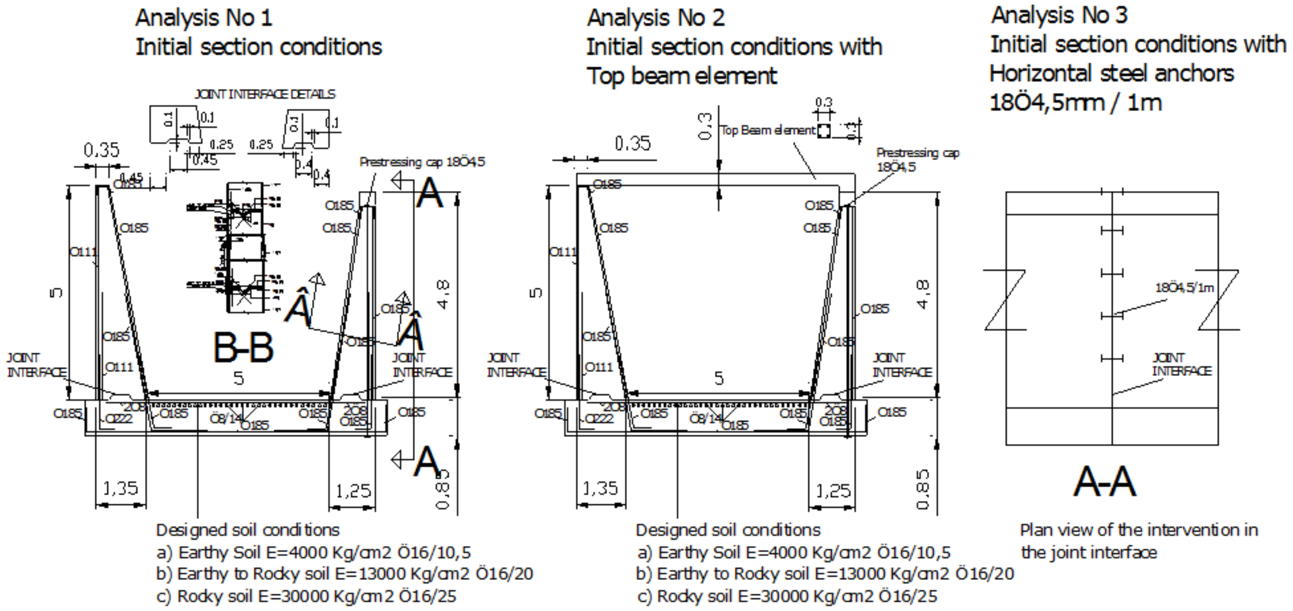


Figure 3: Typical reinforcement details of the canal section in the area of failure *distances cm.

## NUMERICAL SIMULATION OF MORNOS AQUEDUCT IN THE ZONE OF FAILURE

The Lusas 14.7 finite element commercial software was utilised to perform the non-linear static numerical analyses of the aqueduct under a combination of vertical and horizontal loadings [4]. The aqueduct's length that suffered the most severe failures and detachments is simulated in this section. The aqueduct length that was considered in this study spans 108 m. The original layout of the aqueduct in the Taxiarches area was utilised for the realisation of the numerical simulation. One load combinations were considered to act on the canal. It was assumed that the high water level was on the surveillance road next to the canal section (4 m). The canal was considered that has failed with a water level of 3 m inside its section. These load combinations that were tested are depicted in Table 3.

Table 3: Load combination acted on the aqueduct.

| A/a | Load combination | PE(KN/m) | PW(KN/m) | BW(KN/m) |
|---|---|---|---|---|
| 1 | High water level on surveillance road | 110 | 112 | 8.33 |

Table 4: Friction and cohesion values recommended by Cl. 6.2.5(2) of Eurocode 2 (2004).

| Surface texture | Friction coefficient, $\mu$ | Concrete cohesion, $c$ (Mpa) |
|---|---|---|
| Smooth or *left as-cast* | 0.60 | 0.2 |
| Transverse roughened | 0.70 | 0.4 |
| Projecting steel reinforcement | 0.60 | 0.2 |

Table 5: Outline of the numerical analyses.

| Aqueduct analysis case | Load combination | Sub-soil conditions under aqueduct | Structural strengthening scheme |
|---|---|---|---|
| Analysis No 1 | High water level on surveillance road | Non-uniform sub-soil | Vertical pre-stressing wires in the right wall (originally failed) |
| Analysis No 2 | High water level on surveillance road | Non-uniform sub-soil | Horizontal joint top beams and vertical pre-stressing wires in the right wall |
| Analysis No 3 | High water level on surveillance road | Non-uniform sub-soil | Vertical and horizontal pre-stressing wires in the right wall |

The friction and cohesion values recommended by Cl. 6.2.5(2) of the Eurocode 2 are adopted for the simulation of the joint interface between aqueduct segments (Table 4) [5]. Each load combination was comprised of simultaneous action of horizontal active thrust PE, the hydrostatic thrust PW, the gravity load of the aqueduct itself and the upward buoyancy thrust BW of the canal section. The horizontal loads PE, PW were acting transversely to the left and right wall of the aqueduct in direction Y-Y. An outline of the numerical analyses that were carried out to evaluate the different strengthening schemes is reported in Table 5.

Non-linear static analyses were performed assuming each load combination acted separately. The R/C aqueduct walls were simulated by thick shell elements that varied in thickness along their height. The non-linear isotropic multi crack failure criterion (Jefferson, A.D. [6]), was also assumed for the simulation of the wall and bed plate segments. Non-linear 3-D joint interface elements have been adopted for the simulation of: a) the joint interface between wall segments; b) the joint interface between left wall segments and bed plate segments; and c) the joint interface between bed plate segments. The right wall was monolithically jointed to the bed plate segment due to the pre-stressing intervention. The aqueduct was assumed to be laying on uniform fill material as it was assumed in the original study, except a small area under segments 6 and 7 that was identified after the failure and it coincides with the over thrusted soil zone as is shown in the displacement vector graph (Figure 2). The canal was pinned in its ends, where it was in contact with intact canal segments (Figures 5, 6 and 7).

The measured displacement pattern of the failed aqueduct sections has occurred after the original displacement and during the soil erosion that followed the outflow of water from the detached joints. The numerical analysis could not identify the rigid body motion of the aqueduct after failure and after the soil erosion of the foundations of the aqueduct. In Table 6, the numerical predicted patterns of displacements are presented for the three different analyses carried out. The results from analyses No 1 and No 3 have shown much greater displacements in comparison with Analysis No 2.

The load combination that predicts the highest magnitudes of displacement is associated with high water table and, therefore, high hydrostatic pressures acting on the exterior wall of the canal are due to the saturated soil conditions. All the non-linear mechanisms were developed in the interface joints between successive segments. This is an additional reason that suggests that failure was a consequence of detachment of joints that was soon followed by leakage of water that caused the vertical displacement (sinking) of the subsoil next to the canal segments in the right hillside of the canal. In that sense, the failure mechanism was predicted successfully by the numerical simulation.

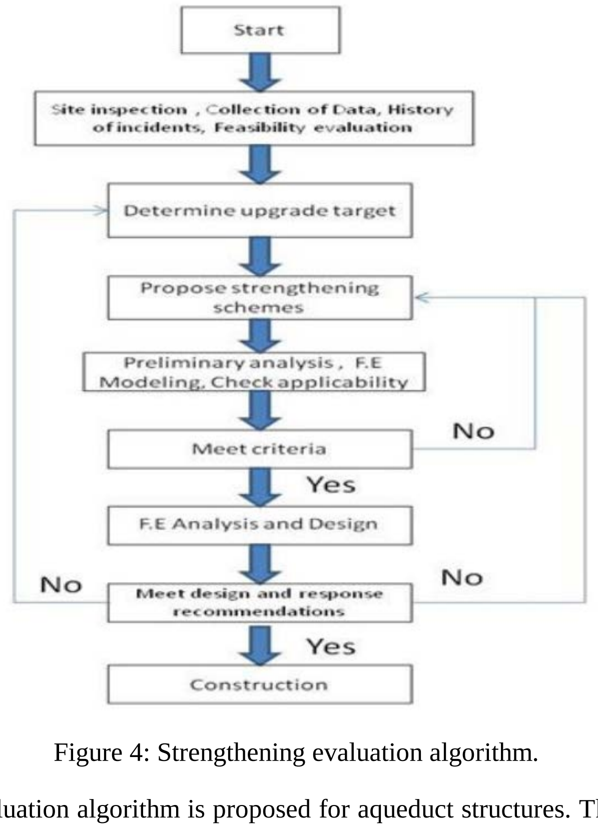


Figure 4: Strengthening evaluation algorithm.

In Figure 4, a strengthening evaluation algorithm is proposed for aqueduct structures. This algorithm was applied in the current investigation. The two strengthening schemes (Analysis No 2 and No 3) are evaluated in respect to the failure pattern (*x* sign) and the non-linear mechanism of the joint interface that is developed in respect to the failure pattern predicted by the actual structural scheme that originally failed (Analysis No 1). The comparison between the failure patterns predicted by the three analyses is shown in Figures 5a, 6a and 7a. The distribution of these failures is most extended in Figures 5a and 5c. The same inspection is carried out for the axial elongation of the interface in Figures 5b, 6b and 7b. Finally, the tensile and compressive in-plane stresses in the walls of the aqueduct for the three analyses can be depicted in Figures 5c, 6c and 7c. The vertical displacements that were approximated numerically were of magnitude of 2.6 mm. Table 6 shows the results of the three analyses.

Table 6: Results of the three analyses.

| No wall segment | Measured displacements (cm) | | Analysis No 1 (cm) | | Analysis No 2 (cm) | | Analysis No 3 (cm) | |
|---|---|---|---|---|---|---|---|---|
| | dx | dy | dx | dy | dx | dy | dx | dy |
| 2 left | -55 | -73 | -1.85 | -4.30 | -0,08 | -0,26 | -1,96 | -4,14 |
| 2 right | -29 | -68 | -0.12 | -0.31 | -0,08 | -0,20 | 0 | -0,30 |
| 3 left | -61.5 | -84 | -4.30 | -9.41 | -0,10 | -0,25 | -4,19 | -8,90 |
| 3 right | -37.5 | -79 | -0.13 | -0.57 | -0,10 | -0,24 | -0.11 | -0,06 |
| 4 left | -63.5 | -86 | -5.62 | -14.6 | -0,10 | -0,26 | -5,02 | -11,90 |
| 4 right | -39.5 | -80 | -0.13 | -0.58 | -0,10 | -0,25 | -0,12 | -0,52 |
| 5 left | -63.5 | -166 | -5.62 | -14.3 | -0,09 | -0,27 | -5,22 | -13,70 |
| 5 right | -66.5 | -109 | -0.13 | -0.56 | -0,09 | -0,26 | -0,11 | -0,51 |
| 8 left | -42 | -20 | -0,22 | -12.2 | -0,22 | -0,44 | -0,22 | -11,80 |
| 8 right | -42 | -20 | -0.66 | -0.15 | 0 | -0,43 | 0 | -0,15 |
| 9 left | -7 | -2 | -0.71 | -6.64 | -0,02 | -0,26 | -0,75 | -6,34 |
| 9 right | -7 | -2 | -0.10 | -0.66 | -0,02 | -0,25 | 0 | -0,63 |

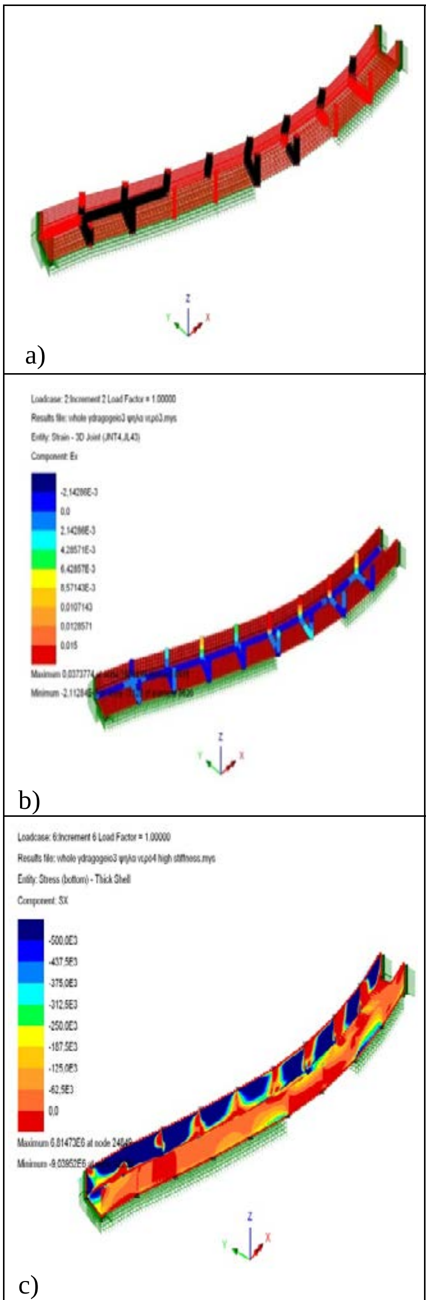


Figure 5: Analysis No 1: a) failure of the joint interfaces; b) axial strain along the joint interfaces; c) in-plane stress contours along wall (bottom layer).

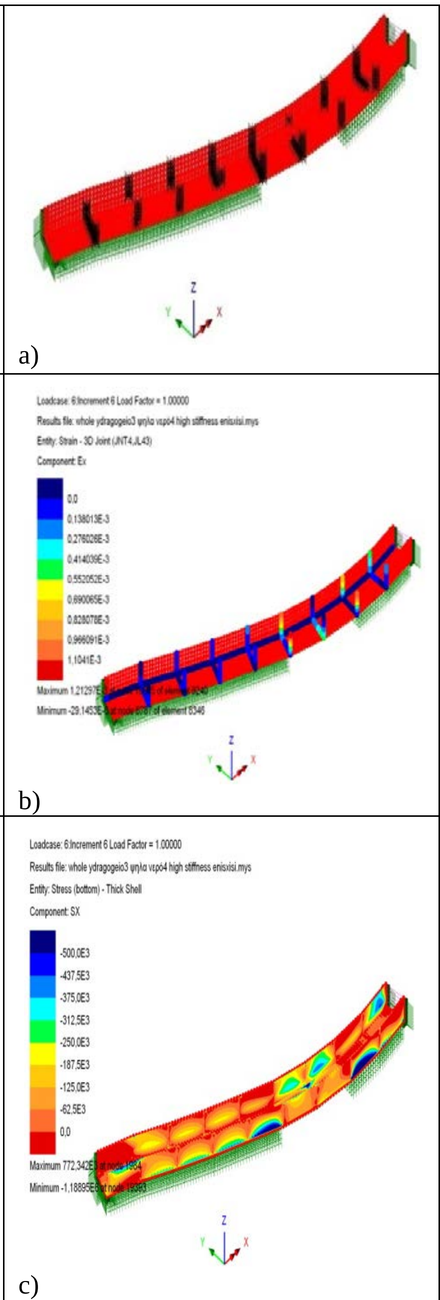


Figure 6: Analysis No 2: a) failure of the joint interfaces; b) axial strain along the joint interfaces; c) in-plane stress contours along wall (bottom layer).

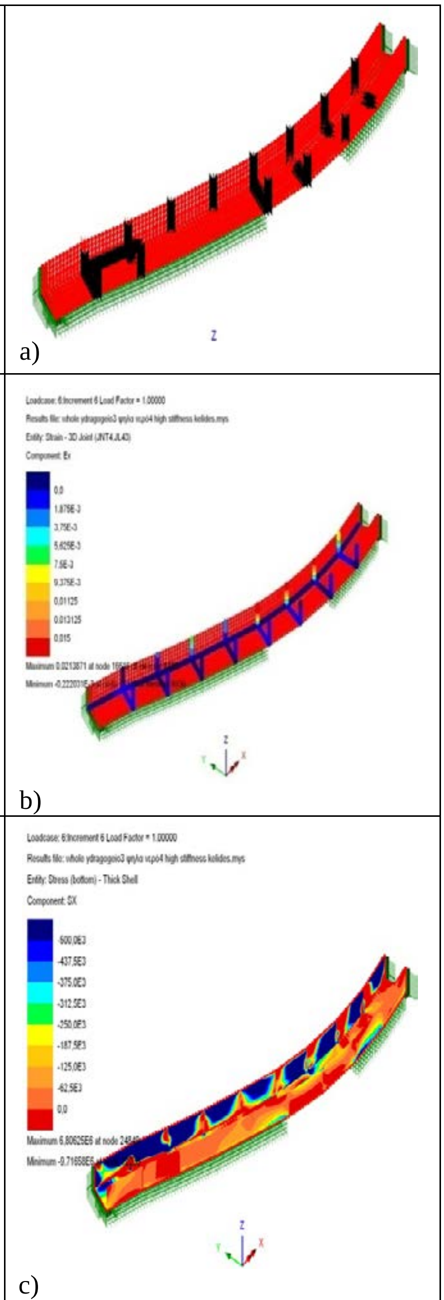


Figure 7: Analysis No 3: a) failure of the joint interfaces; b) axial strain along the joint interfaces; c) in-plane stress contours along wall (bottom layer).

## CONCLUSIONS

The methodology adopted for the investigation of the failure mechanism that was developed numerically predicts deformation patterns that are greater in the area of the maximised curvature of the aqueduct's length under study. This finding agrees with the deformation pattern of the failed aqueduct as shown in Figure 2.

The proposed analysis can be used as a useful design tool in order to assess the structural performance of canal sections and existing aqueducts of the Athens Water Supply System. The current study shows the numerical investigation of three strengthening schemes (one existed) and their behaviour when these structures are situated in areas with poor sub-soil conditions or in areas with variations of sub-soil conditions. A strengthening algorithm is proposed for the evaluation of the structural performance of strengthening schemes for existing aqueducts.

The placement of beam elements that join the sides of the aqueduct as assumed in Analysis No 2, led to reduced failures in the joint between segments, reduced strain elongation in the same joints and lower in-plane tensile stresses at the aqueduct's walls in comparison with the predictions of Analysis No 1 and Analysis No 3. The placement of steel horizontal anchors at the joint between vertical joints (Analysis No 3) although they have beneficial impact in respect to the overall performance, when it is compared with the behaviour predicted by Analysis No 1, they also predict openings, strain elongations in the joint interfaces and tensile stresses in the walls of the aqueduct (Figures 4, 5 and 6). In such way, unfavourable openings in the joints between segments are predicted.

## REFERENCES


1. Kotzias, P. and Stamatopoulos, A., Inspection Report on Aqueducts and Siphons. 4, March (1990).
2. Mourtzas, N.D., Gkiolas A., Vakiris D. and Soulis V., Investigation and mitigation of a failure at the Taxiarches canal of Mornos Aqueduct. Bulletin of the Geological Society of Greece, XLVII 2013, *Proc. 13th Inter. Cong.*, Chania, September (2013).
3. El Dorado Irrigation District (2002), Report *Project 184: Canal Failure Frequency and Analysis*, 4 September (2002).
4. LUSAS 14.7, Finite Element System, FEA Ltd, Kingston, UK (2011).
5. Eurocode 2: Design of concrete structures - Part 1-1: General rules and rules for buildings EN 1992-1-1, Brussels (2004).
6. Jefferson, A.D., A two and three-dimensional multi-crack model for finite element analysis of concrete structures. Submitted to *Computers and Structures*, Aug (1998).


## BIOGRAPHIES

Vassilios Soulis graduated with Bachelor of Civil Engineering from the University of Portsmouth, UK, with an honours degree in 1997. He received a Master's degree from the University of Surrey, UK, in structural engineering. His dissertation was on the seismic behaviour of a four-story building designed as a composite and as an R/C structure. He was then enrolled in the postgraduate programme in the Aristotle University of Thessaloniki, Greece, that has led to a PhD degree on the *Investigation of the Numerical Simulation of Masonry Infilled R/C Frame Structures under Seismic Type Loading*. He is a supervisor engineer in the Athens Water Supply and Sewerage Company. He has been involved in over 40 major hydraulic engineering projects. He is also a lecturer in seismic design and dynamic analysis of structures at the School of Pedagogical and Technological Studies in Athens, and is a visiting lecturer at Piraeus University of Applied Sciences in the module of Legal and Contractual Obligations. He has over of 60 articles peer-reviewed and published in international and Greek journals and conferences.

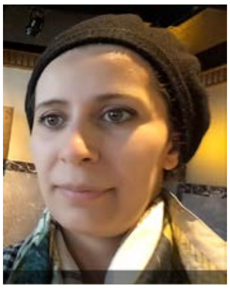

Randa Hattab is a civil engineer with extensive experience in all *civil project* phases, experienced in design, supervision and project execution. She graduated from An-Najah National University. Her current engagement is in the MSc degree in structural design and construction management in order to advance her research experience in addition to experiencing new market trends, methods and technologies in construction business. She is an inspirational and solution oriented team player with a natural sense of urgency and the ability to anticipate, identify and respond to changing business priorities, demonstrating solid interpersonal communication skills and capable to achieving all company goals and objectives.